An intercomparison of global oceanic precipitation climatologies

Graham D. Quartly,[1] Elizabeth A. Kyte,[1,2] Meric A. Srokosz,[1] and Michael N. Tsimplis[1]

[1] Large-scale patterns of precipitation are important for the changes they may effect upon the circulation of the ocean. However, marine precipitation is very hard to quantify accurately. Four independent climatologies are examined to compare their estimates of the annual mean precipitation, and the seasonal and interannual variations. One data set, Global Precipitation Climatology Project (GPCP), is based upon satellite data, the other three on output of weather forecast reanalyses from the National Centers for Environmental Prediction (NCEP) and the European Centre for Medium-Range Weather Forecasts (ECMWF). Although all data sets have their errors, there is general agreement on the geographical patterns of precipitation. All the models had higher rain rates in the tropics than shown by the satellite data, and also greater seasonal ranges. However, GPCP has 10–25% more precipitation than NCEP and ECMWF in most of the southern regions, because of their weak representation of convergence zones; NCEP2, a more recent version of the NCEP reanalysis, shows a marked improvement in this area. However, in most regions NCEP2 exhibits a larger seasonal range than shown by other data sets, particularly for the Tropical Pacific. Both NCEP and NCEP2 often show a seasonal cycle lagging 2 months or more behind GPCP. Of the three reanalysis climatologies, ECMWF appears best at realizing the position and migration of rain features. The interannual variations are correlated between all four data sets; however, the correlation coefficient is only large for regions that have a strong response to El Niño and La Niña events, or for comparisons of the two NCEP reanalyses. Of the data sets evaluated, GPCP has the most internal consistency, with no long-term trend in its regional averages, and it alone shows the deficit in Mediterranean precipitation coincident with the Eastern Mediterranean Transient.

Citation: Quartly, G. D., E. A. Kyte, M. A. Srokosz, and M. N. Tsimplis (2007), An intercomparison of global oceanic precipitation climatologies, *J. Geophys. Res.*, *112*, D10121, doi:10.1029/2006JD007810.

1. Introduction

[2] The net freshwater flux between atmosphere and ocean is an important climatic quantity. Changes in its value may act as an indicator of climate change, but also long-term variations in the atmosphere-ocean exchange may act as the mediator of climate change through their effect upon the salinity of surface waters and consequently on the overturning density-driven circulation. The net flux is the difference between precipitation and evaporation; here we investigate the magnitudes and variability of the precipitation component using four different quasi-global data sets. Our aim is to identify internal inconsistencies within these climatological data sets, to quantify the mean and seasonal variations within them, and to assess their appropriateness for freshwater forcing of ocean models. In this paper we note the many similarities between the data sets, which provide confidence that the results reflect the true state of global precipitation; however, we also seek to identify and characterize the differences between the data sets, and attempt to apportion error. We offer some suggestions as to the physical causes of these discrepancies, but leave the detailed attribution to those more versed in inversions of satellite data or precipitation parameterization in models. By focussing on large areal averages, we seek to examine the usefulness of these data sets in providing one component of the freshwater forcing for ocean models. In the context of ocean models, the precise positioning of rain belts is not important, rather it is the actual quantity of fresh water being added to the surface ocean in a given region. By characterizing and fully understanding the errors in these various data sets, the aim of the precipitation community is to develop a consistent and accurate climatology, using the strengths of each of its component sources.

[3] A number of papers have compared the mean precipitation from various climatologies, in terms of both their geographical distributions [*Huffman et al.*, 1997; *Kidd*, 2001; *Adler et al.*, 2001] and by showing zonal averages to highlight the differences in magnitude [*Taylor*, 2000]. Here we examine the data for ten separate ocean regions, looking not just at the mean rainfall within different clima-

---

[1]National Oceanography Centre, Southampton, Empress Dock, Southampton, UK.
[2]Now at School of Ocean Sciences, University of Bangor, UK.

tologies, but also at the magnitude of the seasonal and interannual variations. This enables us to see how consistent the various climatologies are in their portrayal of unusual climatic conditions. As ocean models use atmosphere-ocean freshwater fluxes prescribed according to certain climatologies, it is important to see how much these differ, both in their annual mean flux and its seasonal variation.

[4] Section 2 introduces each of the data sets in turn, including some discussion of their evolution and internal changes. In section 3, we determine time series of data from the four climatologies for their common period, and resolve these into seasonal cycles plus interannual anomalies. We provide a particularly focused investigation of two important regions, the Mediterranean and the Tropical Atlantic, showing the differences in the positioning of the rain region within the various data sets. The former is a critical area because it contains regions of deep-water formation (Gulf of Lyons and Aegean/Adriatic Seas). The Tropical Atlantic is a complex region with an annual shift both meridionally and zonally in the region of convective activity, and it is the region in which the hurricanes that reach the eastern US coast develop. Section 4 discusses the differences and agreements between the four data sets, with the key findings provided in a summary. A companion paper [Kyte et al., 2006] looks at the differences in the spatial representations of El Niño and North Atlantic Oscillation within these climatologies. Our attention was recently drawn to a paper by Béranger et al. [2006] who compare many precipitation data sets for the period 1980 to 1993, using some similar analysis. Our paper differs from theirs in that it uses four data sets of more than 20 years duration, specifically including the latest reanalysis fields (NCEP2 and ECMWF 45-year reanalysis, see below), and that our averaging areas encompass the full movement of the rainbands in the equatorial Atlantic and Pacific.

2. Data Sets Used and Their Internal Inconsistencies

[5] Four data sets are used, each of more than 20 years duration, with near global coverage over land, sea, and ice. They are all widely available and have thus been used individually in many research publications. Here the comparisons are for the common overlap of 1979–2000. Some of the data sets are of longer extent; however, we focus on the changes during the common 22-year period. All rain rates are expressed as equivalents for 30-day months, so that the different lengths of months have no impact upon the appearance of the seasonal cycle.

2.1. GPCP

[6] A number of different precipitation data sets have been produced by the Global Precipitation Climatology Project; we use here the multisatellite product, which melds together information from a number of different satellite sensors, but does not include any output from weather forecast models. The data are available as monthly fields on a $2.5° \times 2.5°$ grid, and the particular product used here is the updated version 2 (released in June 2006), acquired from the Goddard Space Flight Center (ftp://precip.gsfc.nasa.gov/pub/gpcp-v2/int/). This latest version is identical to the original version 2 over the ocean, but has had all land and coastal data modified for dates since 1987 to bring them into closer agreement with the 1979–1987 epoch and with land-based rain gauges (D. Bolvin, personal communication, 2006). This change has led to both moderate increases and decreases in rainfall depending upon the land region. There are a number of different satellite sensors that can yield rain records, but their measurements relate to different aspects of the rain systems [Quartly et al., 2002]. Thus, care is required in merging the disparate contributions with differing spatial coverage and temporal span. This information is detailed in the work of Huffman et al. [1997], Adler et al. [2003], and Huffman and Bolvin [2004].

[7] During the period of interest a number of major changes occurred that affect the precipitation estimates. Data from the Special Sensor Microwave/Imagers (SSM/I) became available from July 1987 onwards (except for December 1987). These microwave sensors on polar-orbiting spacecraft improved the sensing of precipitation especially in high latitudes. Data from the TIROS Operational Vertical Sounders (TOVS) have been available since 1979, but in the GPCP processing they are used in conjunction with SSM/I data, and so are only utilized after July 1987. The two 85.5 GHz channels on the first SSM/I failed during 1990–1991 necessitating a change in the algorithm applied. The orbits of polar-orbiting craft are not always tightly constrained, and so may gradually drift, thus making observations at different times of the day. Subsequent switching from one "operational SSM/I" to another may also affect mean derived rain rate due to different diurnal sampling or different errors in the calibration of its channels.

[8] Prior to the arrival of SSM/I, estimates of precipitation in high latitudes were based on Outgoing Longwave Radiance (OLR) estimates computed from infrared data from low-earth orbit (LEO) satellites. Infrared sensors on geostationary (GEO) satellites were added to the arsenal in 1986, but these could not provide useful precipitation estimates at latitudes poleward of $40°S$ and $40°N$. Also, there was incomplete geostationary coverage of the tropical regions until Meteosat-5 was placed over the Indian Ocean in June 1998. The major volcanic explosions of El Chichón (1983) and Pinatubo (1991) may have an effect: Mass and Portman [1989] suggests that the extra stratospheric aerosols have no long-term impact upon the precipitation, but these atmospheric contaminants might cause biases in retrieval algorithms for visible and infrared sensors. Figure 1 summarizes the various internal changes and problems in each of the data sets used in this investigation.

[9] This data set is one of several possible choices for a satellite precipitation climatology. It is also one of the most widely used for climatic analysis, but that does not imply that it is perfect. Other climatologies based on single or multiple sensor syntheses do yield different mean levels of tropical and midlatitude rain; a review of the intercomparison of satellite products is provided in section 4.1.

[10] Although considerable effort has been made to merge the data in a manner yielding a consistent long-term data set [Huffman and Bolvin, 2004], some changes can be discerned. Prior to the advent of SSM/I and TOVS, oceanic rain rates were based on OLR data, which respond to the conditions of cloud tops rather than the precipitation itself. Although the SSM/I- and OLR-based estimates have been adjusted so that the monthly means are roughly the same,
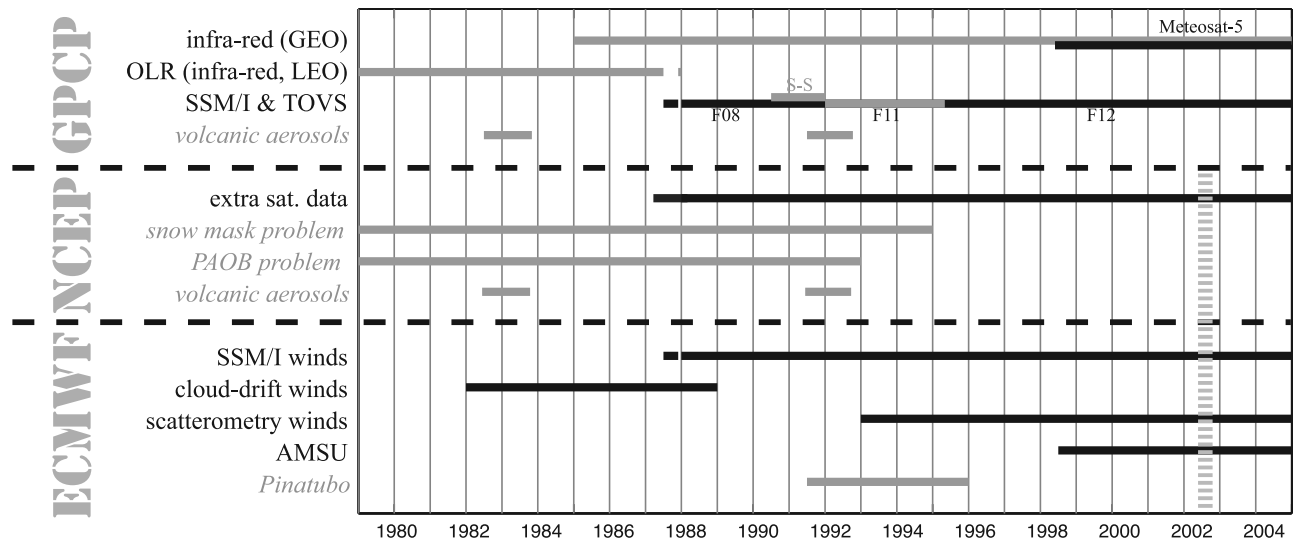
Figure 1. Factors possibly affecting the consistency of precipitation climatologies. The items labeled in dark type represent sources not contributing for the whole period, whereas the light type indicates problems that arose. Labels on x axis mark starts of years. F08, F11, and F13 are individual spacecraft and S-S is when SSM/I scattering algorithm had to be used; for further explanation of terms in this figure consult the relevant parts of section 2. The vertical dashed line marks the end of the ECMWF dataset (August 2002) and the end of our holding of the first NCEP reanalysis (July 2002).

the infrared-only data show less month-to-month variations. As an illustration, we examined the mean precipitation in two small boxes (North Atlantic and North Pacific) outside the coverage of geostationary infrared, and where midlatitude storm systems can give great variations in rainfall. Each series was divided into 1979–1986 (8 years of pre-SSM/I)

and 1988–2005 (18 years of post-SSM/I), with seasonal cycles and anomalies relative to them calculated separately for each part. The interannual anomalies are ~50% bigger during the second period than the first (Figure 2) as the cloud cover is less variable than the actual occurrence of active rain events.
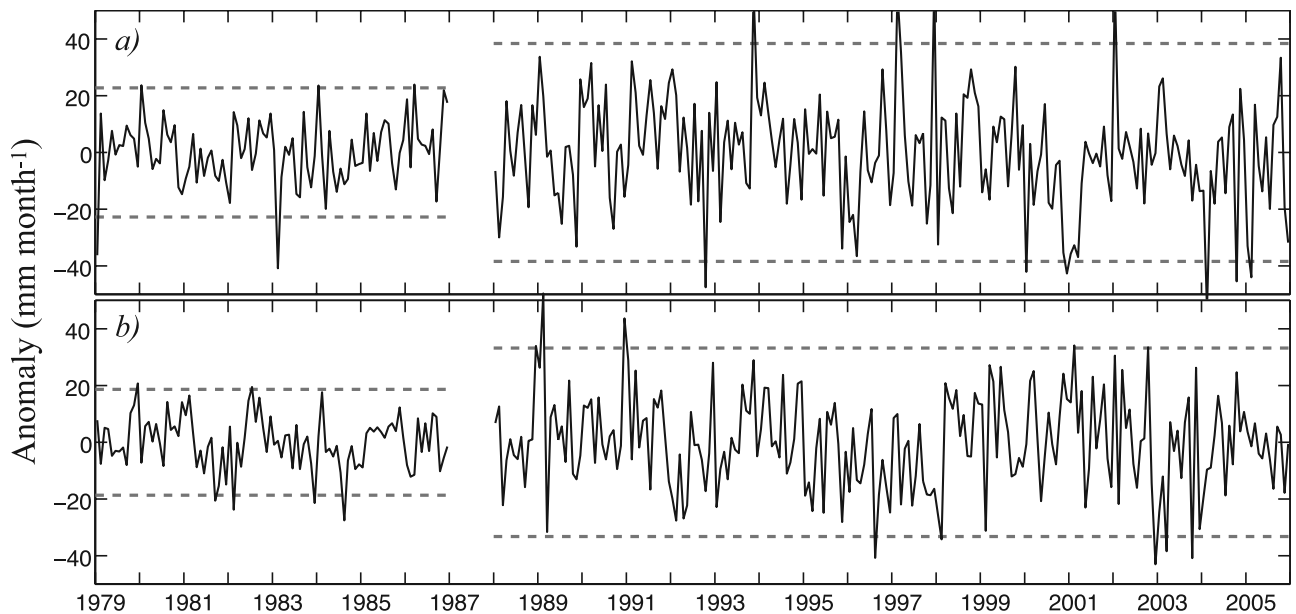

Figure 2. Example of change in variability of GPCP for midlatitudes after SSM/I data are incorporated in July 1987. Plot is of monthly anomalies calculated separately for the two epochs, with dashed lines showing ±2 standard deviations (SD). (a) North Atlantic box is 45°–60°N, 35°–15°W: SD changes from 11.4 to 19.2 mm month^{-1}; (b) North Pacific box is 45°–60°N, 180°–210°E: SD changes from 9.3 to 16.6 mm month^{-1}. Tick marks on ordinate mark start of each year.
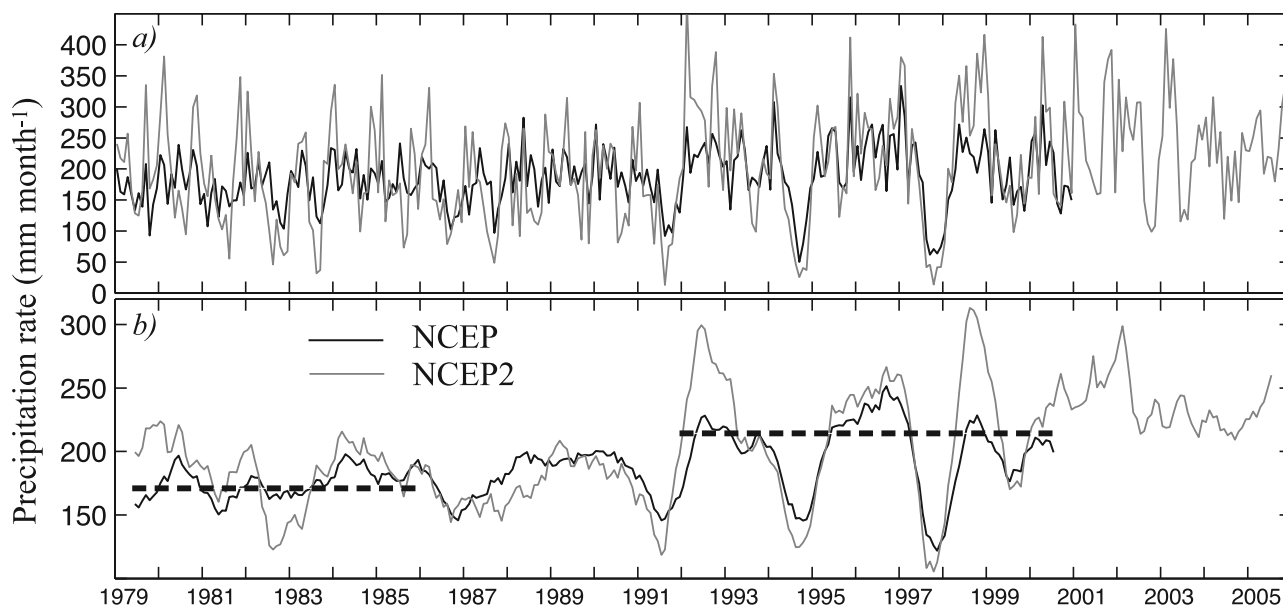
Figure 3. Time series of NCEP and NCEP2 rainfall in southern tropical Indian Ocean (80°–105°E, 15°–5°S). (a) Individual monthly values showing greater short-term variability in NCEP2; (b) Same after smoothing with 11-month running mean, showing the greater long-term extremes in NCEP2. Heavy dashed lines indicate mean values for NCEP for pre-1986 and post-1991 periods; both data sets show increased rainfall in the latter period compared with the earlier one. Tick marks on ordinate mark start of each year.

2.2. NCEP

[11] The second data set we use is derived from a reanalysis of global meteorological observations by the US National Centers for Environmental Prediction (NCEP) and National Center for Atmospheric Research. Their aim was a consistent assimilation of observations from 1949 onwards into a model of the atmospheric circulation and humidity. Rain observations themselves are not used, as it is difficult to assimilate such data; the rain rate is inferred from other aspects of the model, and is thus completely independent of the rain observations used for the GPCP data set. The NCEP product (up to July 2002) was obtained from http://ingrid.ldeo. columbia.edu/SOURCES/NOAA/NCEP-NCAR/CDAS-1/ MONTHLY/outline.html as monthly files on a 1.875° × 1.905° grid and interpolated by us to a 2.5° × 2.5° grid. The latter process will have caused a slight blurring of sharp regional features in the precipitation pattern, but not significantly affected averages over ocean regions. Full details on the model reanalysis are given by *Kistler et al.* [2001] who noted that the full reanalysis period could be divided into three major epochs according to the nature of the observations being incorporated.

[12] The last phase (1979 onwards) corresponds to the inclusion of satellite data, and here we are only concerned with data from that period. The advent of more satellite data in 1987 does significantly increase the number of observations (see Figure 1 of *Kistler et al.*, 2001), but as rain records from these sensors are not assimilated, the effect upon the determination of model rainfall is less noticeable than for GPCP. *Kistler et al.* [2001] discuss two changes in processing that relate to the satellite era. First, an incorrect mask for snow cover was used until 1994, but this error principally affected the North American landmass. Second,

there was a longitudinal location error of 180° in PAOBs (sea level pressures from manual analyses) that was rectified in 1993; however, the effect upon the derived circulation was only significant south of 40°S. The effect of these changes is not easily discernible in regional averages of precipitation.

[13] Figure 3 shows the mean areal rainfall for a region of the eastern tropical Indian Ocean. There are three marked reductions in rainfall in late 1991, mid-1994 and late 1997. These events, occurring in the second half of the years mentioned, correspond to anomalously northward migrations of the intertropical convergence zone (ITCZ), such that it has little overlap with the selected box. These might be a consequence of El Niño events (although that in 1994 was by all measures a weak one); however, the changes in late 1982 and late 1986 are muted by comparison. Disregarding these extrema, the mean rainfall rate for this region shows a marked increase, from around 165 mm month^{-1} for pre-1986 records to ∼210 mm month^{-1} for 1992 onwards.

2.3. NCEP2

[14] More recently, output from a further run of the NCEP model has become available from the National Climatic Data Center (http://www.ncdc.noaa.gov/oa/ncdc.html). These data were produced for the Atmospheric Model Intercomparison Project (AMIP-II) [*Kanamitsu et al.*, 2002], are on the same grid as the original NCEP analysis, and span from 1979 to the present day; data up till the end of 2005 were used here. There is a major change between the NCEP reanalysis and the NCEP2 reanalysis. Not only were all the errors mentioned in the previous subsection removed, but also a number of improvements were made to the model physics. These included reducing ocean albedo
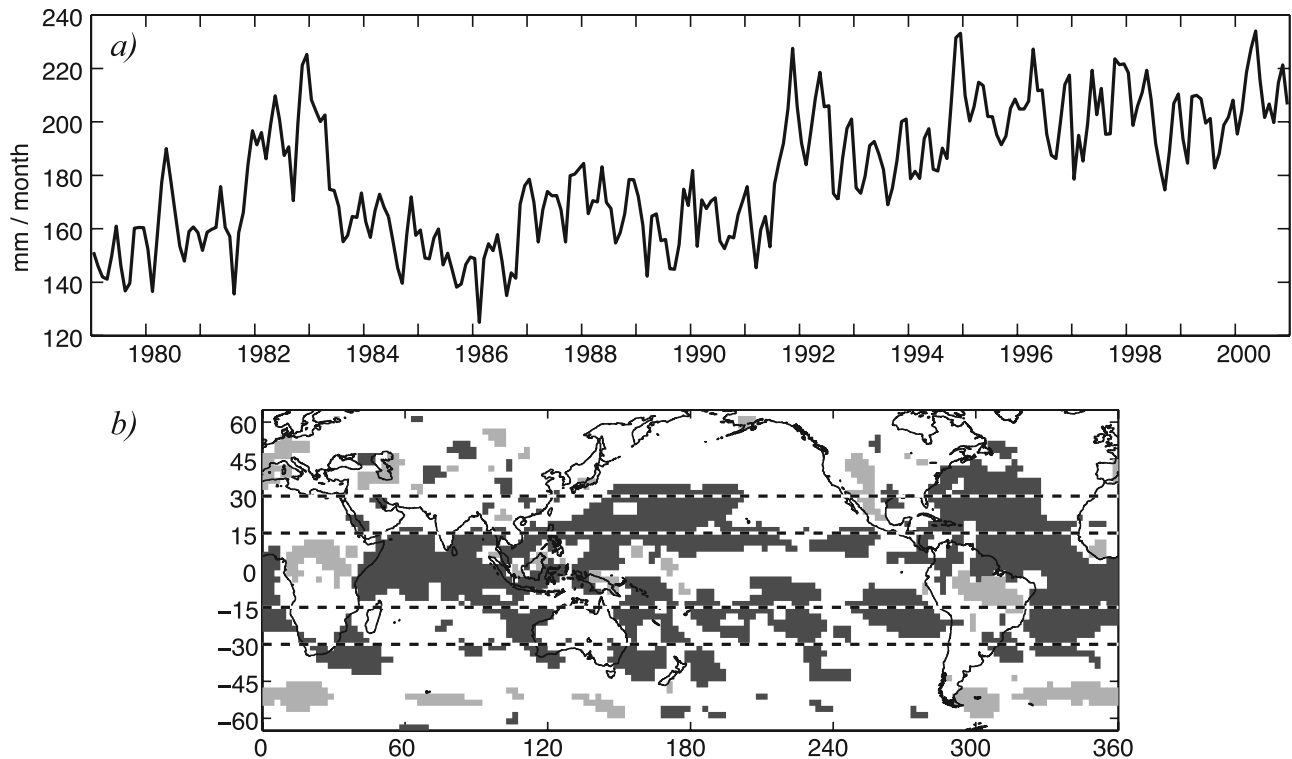
Figure 4. (a) Time series of oceanic rainfall within ECMWF, averaged over 15°S to 15°N. Tick marks on ordinate mark start of each year. (b) Individual pixels for which ECMWF precipitation shows a trend during 1979–2000 that is statistically significant at the 95% confidence level. Dark shading indicates an increase; light shading a decrease.

by more than 50%, changing the short-wave flux model to reduce surface insolation, increasing the outgoing long-wave radiation thus enhancing cloud top cooling, and applying modified parameterizations for stratus clouds and for convection. These are all expected to impact on the precipitation rate [*Kanamitsu et al.*, 2002]. As will be shown later, one effect is to increase the precipitation rate substantially in some regions; in our example region in the Indian Ocean it also greatly increased the variability on both a month-to-month basis (Figure 3a) and heightened the maxima and lowered the minima seen on a yearly timescale (Figure 3b).

2.4. ECMWF

[15] A separate global weather forecast model is run by the European Centre for Medium-Range Weather Forecasts (ECMWF). Again, this assimilates a wide variety of meteorological records (but not including precipitation itself). However, the model has a different resolution and number of layers than NCEP, includes some different observations (wind fields from scatterometry, and the direct assimilation of raw microwave radiance data) and uses a three-dimensional variational assimilation scheme [*Uppala et al.*, 2004]. The 6-hourly data from the ECMWF reanalysis were obtained from http://data.ecmwf.int/data/d/era40_daily/ and composited to monthly files. We then reinterpolated the data from their interpolated 2.5° × 2.5° grid on to the same 2.5° grid as the other data sets being analyzed.

[16] Although a consistent model was used for the whole duration of the reanalysis (September 1957 to August

2002), there are various problems associated with changes in the observing system. Some of these correspond to the addition of new sensors, but there are also geophysical problems such as the aerosol loading resulting from the explosion of Pinatubo affecting radiance measurements from mid-1991 to 1996. Satellite-derived winds are an important tool in locating regions of surface convergence and quantifying the convective activity. A reprocessing of Meteosat data from 1982 to 1988 gave information on the wind field at various heights through the tracking of drifting clouds. Wind vector data from scatterometry started being utilized from 1993 onwards. However, the increasing use of humidity profiles from satellite-borne sounders has led to the increased occurrence of supersaturated air and consequent precipitation. *Hagemann et al.* [2005] attribute this to a problem with the assimilation of humidity data into the model. This problem is most pronounced in the tropics, and increases with time as the density of satellite humidity observations increases. More details on the changes in the source data are described by *Uppala et al.* [2004].

[17] The effect of the increased density of humidity observations is illustrated in Figure 4a, which shows that the mean oceanic rainfall between 15°S and 15°N is much greater in the last 10 years than the previous 12. *Troccoli and Kållberg* [2004] offer an adjustment by rescaling the precipitation between 30°S and 30°N to give the same net freshwater flux as obtained in earlier epochs, while maintaining a precipitation field consistent with a climatology based on GPCP data for 1979–2000. We have not used such an adjusted data set, because that takes away some of
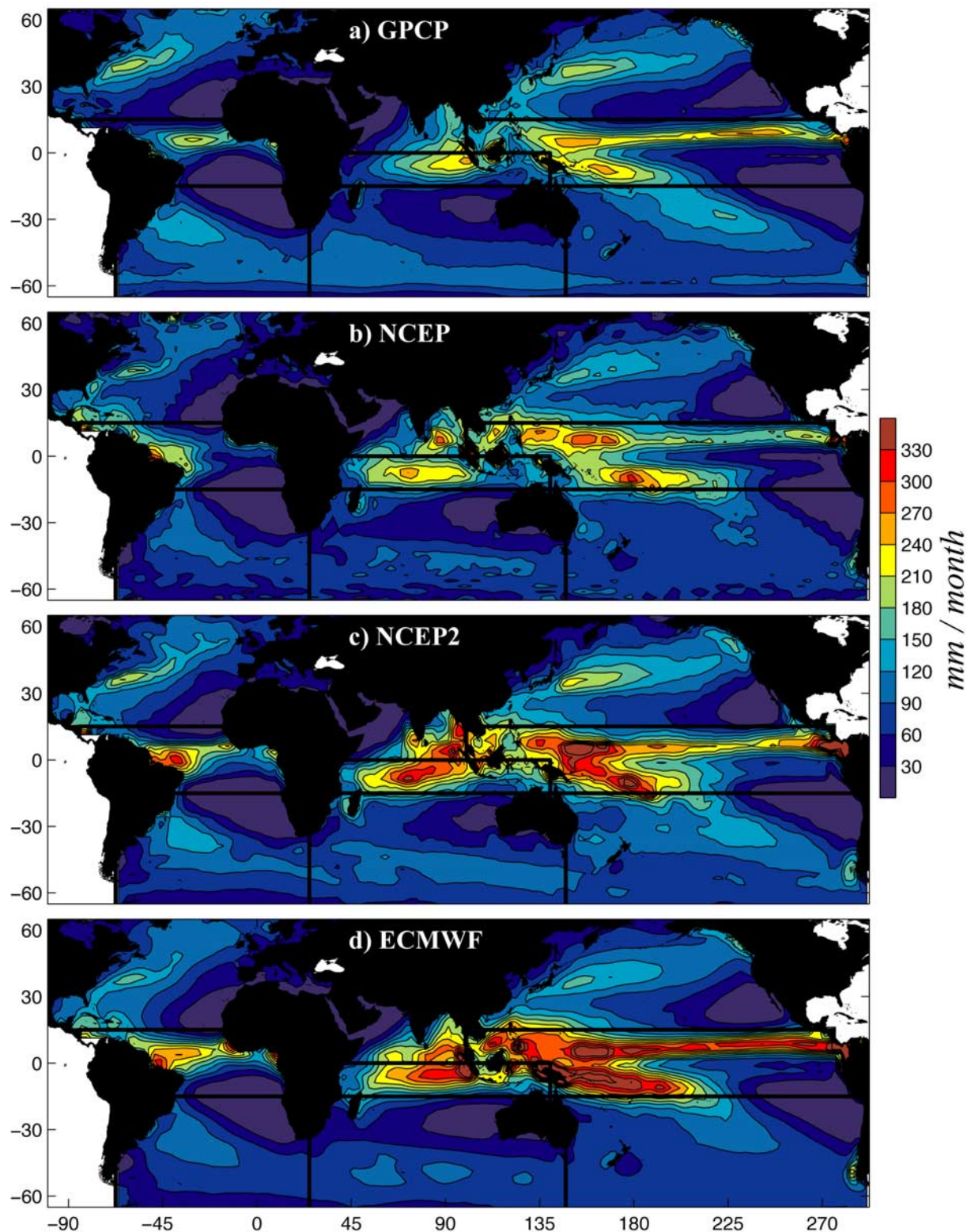
Figure 5. Mean precipitation fields for the entire 1979–2000 period for (a) GPCP, (b) NCEP, (c) NCEP2, and (d) ECMWF. For analysis, these are subsequently divided into the ten regions shown: the Mediterranean, plus three regions for each of Atlantic, Indian, and Pacific. Dividing zonal lines are at 15°S and 15°N (0°N in the Indian Ocean), with meridional lines at 67.5°W, 25°E, and 147.5°E (100°E between North Indian and Tropical Pacific). The North Sea and Hudson Bay contribute to the North Atlantic, and the Red Sea to the North Indian, but the Black Sea is not incorporated in our definition of the Mediterranean because the flow linking them is so weak.
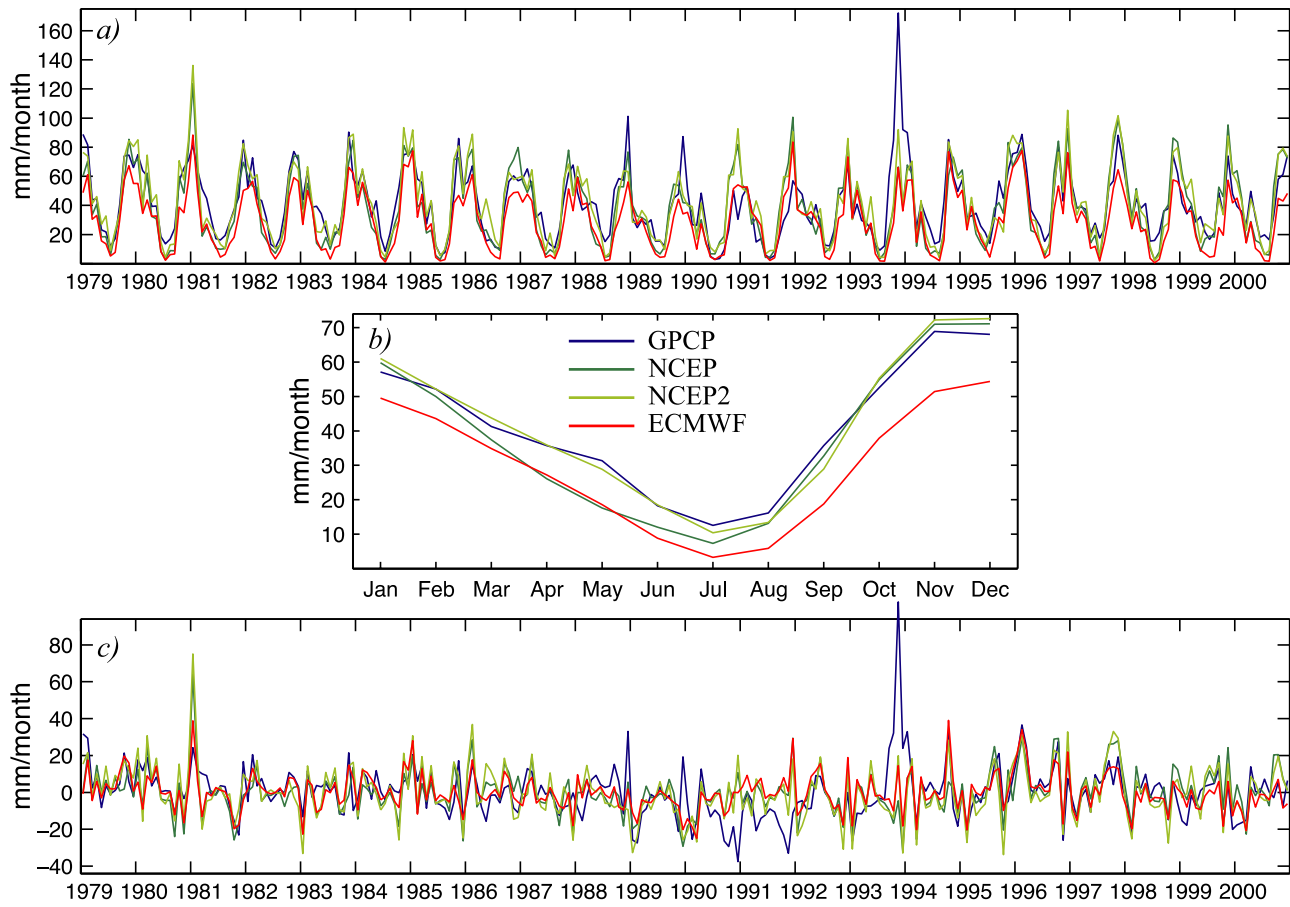
Figure 6. Example of time series of precipitation within the three climatologies for the Mediterranean. (a) Monthly rainfall values. (b) Mean for each calendar month. (c) Anomalies for each month. Labels on x axes of (a) and (c) mark start of years.

the independence with respect to the GPCP data, and artificially removes any long-term temporal changes. Besides, the advocated correction is zonally invariant, whereas the gradual increase is only significant over the ocean, and then not equally so at all longitudes. Figure 4b highlights all those pixels showing a statistically significant trend within the ECMWF precipitation data set, which clearly reveals increases in the western Atlantic between 35°S and 45°N and also that there are apparent reductions over the tropical rain forests of Amazonia and Central Africa. However, this known problem with the ECMWF precipitation data should be borne in mind when studying later results.

3. Regional Comparisons

[18] Notwithstanding the various inconsistencies within the individual data sets, we have chosen to compare them using the full period in common (1979–2000). The mean geographical patterns for our data sets are illustrated in Figure 5. Many authors have displayed such mean climatologies; here we draw especial attention to the more intense Pacific ITCZ (intertropical convergence zone) in ECMWF, the near-zonal SPCZ (South Pacific convergence zone) in models (noted previously by *Taylor*, 2000), and that GPCP shows more pronounced midlatitude features in both hemispheres. Because of our interest in the modification of

surface water masses, we are very much concerned with large-scale variations rather than the changes at a specific locality. Thus we define ten regions for quantitative study (Figure 5), with the zonal boundaries for the tropical regions being sufficiently wide to include the range of latitudes of the ITCZ. For each region, we determine average precipitation values by weighting the contribution of individual grid boxes according to their area (effectively dependent upon the cosine of the mean latitude). From the 264-month time series, we calculate a mean for each calendar month (January, February, etc.) and remove these monthly means to leave precipitation anomalies for each month.

[19] We illustrate this analysis first of all for the Mediterranean (Figure 6). As there are relatively few 2.5° × 2.5° pixels within it that are ocean-only, we have expanded the set of points considered to include all those that are predominantly marine (i.e., less than 50% land). This is not a typical basin, in that it has the most marked seasonal cycle, but its use as an introductory example makes it easier to contrast the results of the others in sections on austral, boreal and central regions. There is a strong similarity between the precipitation rates in all four data sets (Figure 6a), with a minimum during June–August, when rainfall is less than 30% of that found in the boreal winter.

[20] Table 1 shows the correlation between the different time series for each of the regions. Each regional time series

Table 1. Correlation Coefficient for Intercomparisons of the Four Different Estimates of Monthly Rainfall for the Ten Regions Plus Global Ocean, and Also for the Correlation of Their Anomalies After Removal of Seasonal Signals[a]

Ocean Region	Correlation of Rainfall Values						Correlation of Rainfall Anomalies					
	GPCP Versus NCEP	GPCP Versus NCEP2	GPCP Versus ECMWF	NCEP Versus NCEP2	NCEP Versus ECMWF	NCEP2 Versus ECMWF	GPCP Versus NCEP	GPCP Versus NCEP2	GPCP Versus ECMWF	NCEP Versus NCEP2	NCEP Versus ECMWF	NCEP2 Versus ECMWF
Mediterranean	**0.80**	**0.82**	**0.84**	**0.96**	**0.93**	**0.94**	**0.39**	**0.47**	**0.54**	**0.90**	**0.82**	**0.84**
North Atlantic	**0.94**	**0.95**	0.80	**0.97**	**0.86**	0.79	**0.52**	**0.57**	**0.42**	**0.88**	**0.63**	**0.62**
Trop. Atlantic	**0.62**	**0.69**	**0.58**	0.58	**0.68**	0.46	**0.55**	**0.55**	**0.56**	**0.72**	**0.56**	**0.55**
South Atlantic	**0.68**	0.62	**0.66**	**0.97**	**0.79**	**0.74**	**0.47**	**0.48**	**0.35**	**0.91**	**0.54**	**0.53**
North Indian	**0.81**	**0.73**	**0.90**	**0.87**	**0.83**	**0.77**	**0.64**	**0.55**	**0.69**	**0.61**	**0.59**	**0.58**
Central Indian	**0.83**	**0.75**	**0.82**	**0.81**	**0.83**	**0.82**	**0.63**	**0.46**	**0.58**	**0.67**	**0.56**	**0.44**
South Indian	0.79	0.69	**0.84**	**0.96**	0.79	0.72	**0.42**	**0.41**	**0.43**	**0.91**	**0.42**	**0.46**
North Pacific	**0.85**	0.73	**0.78**	**0.93**	0.69	0.48	**0.62**	**0.58**	**0.54**	**0.90**	**0.70**	**0.67**
Trop. Pacific	**0.69**	**0.63**	**0.63**	**0.75**	**0.63**	**0.57**	**0.73**	**0.70**	**0.63**	**0.81**	**0.63**	**0.66**
South Pacific	**0.77**	**0.74**	**0.78**	**0.95**	0.72	0.70	**0.58**	**0.60**	**0.55**	**0.90**	**0.58**	**0.58**
Global Ocean	0.21	0.07	0.17	**0.69**	0.29	0.30	0.32	0.33	0.10	**0.74**	0.28	0.40

[a]All statistics calculated over the common period, 1979–2000, with trends removed beforehand. Results that are statistically significant at the 95% level are shown in bold.

was detrended first (to avoid biasing by the long-term changes shown for ECMWF (Figure 4) and noted in section 3.3 for other regions/data sets. Although each time series consisted of 264 monthly maps, the number of degrees of freedom is less because of serial correlation. We estimated the appropriate value for each pairwise comparison using the autocorrelation functions for the two series, following the approach of *Yin et al.* [2004]. Correlations that are significant at the 95% level (student *t* test) are shown in bold in Table 1.

[21] The correlation coefficients for the comparison of GPCP with NCEP, NCEP2, and ECMWF are 0.80, 0.82, and 0.84, respectively, with the correlation between the various reanalyses being at least 0.93. A good part of the

noted similarity is due to the common seasonal cycle, with GPCP and ECMWF sharing the same seasonal variation (Figure 6b), but the satellite-derived values being greater by 4 to 18 mm month^{-1}. The NCEP data have a larger seasonal range, with close agreement with GPCP during August to January, but being on average 10 mm month^{-1} less during the other 6 months. The revisions to the NCEP reanalysis have increased the precipitation in the first half of the year, without changing those for July to December. The result is a very close match with GPCP in terms of seasonal cycle. These seasonal variations can be contrasted with the outflow in various catchment areas. *Struglia et al.* [2004] noted that the discharge of Mediterranean rivers peaks in March
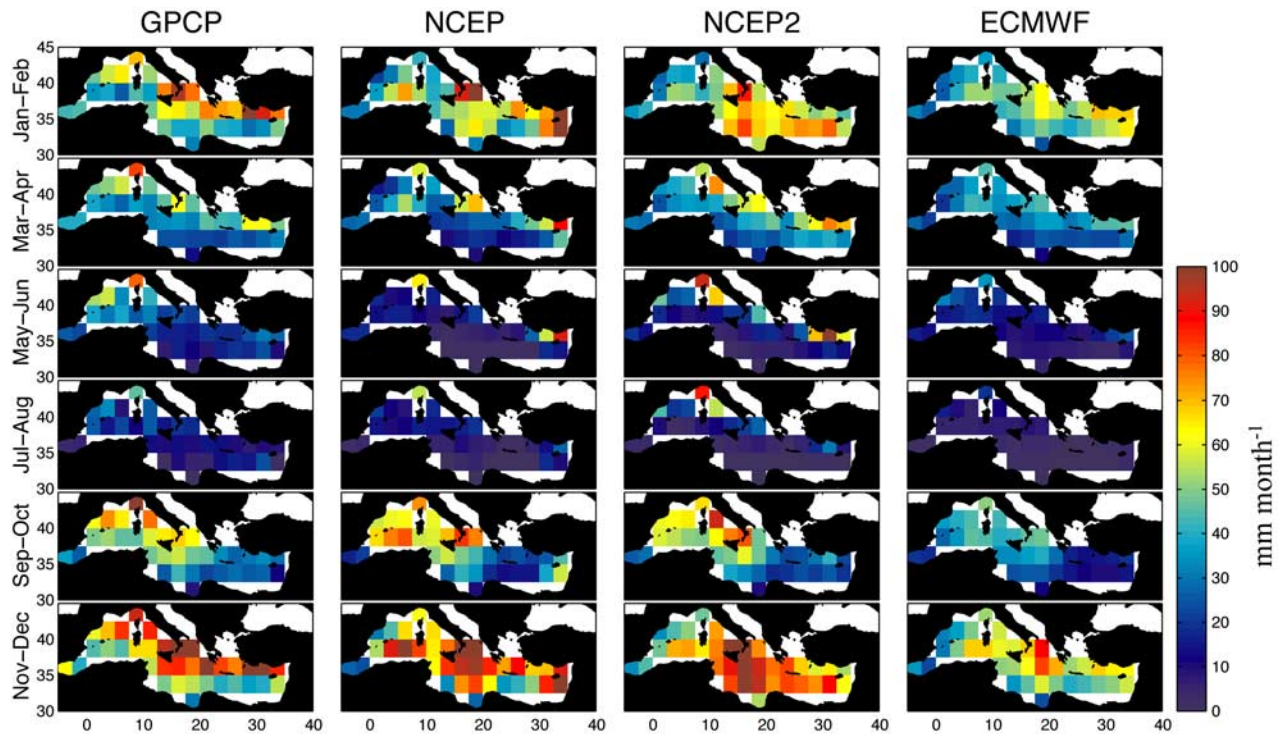

Figure 7. Comparison of seasonal variations in the Mediterranean, with mean climatologies shown for each 2-month period.
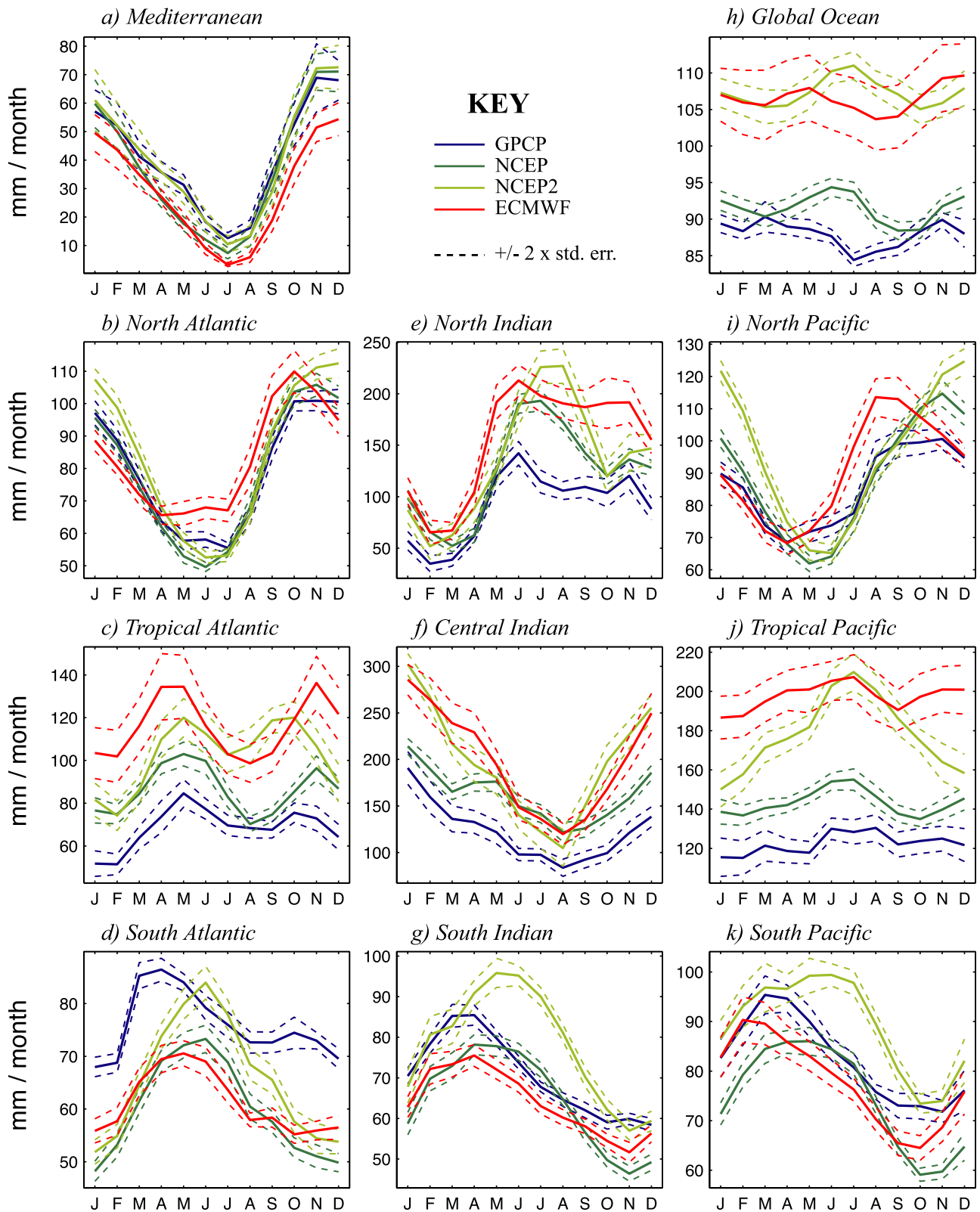
Figure 8. Monthly means for each of the chosen regions. The dashed lines show the uncertainties in each monthly mean (±2 times the standard error). Note different scales are used for each plot to enable the seasonal variations and differences between data sets to be seen clearly.
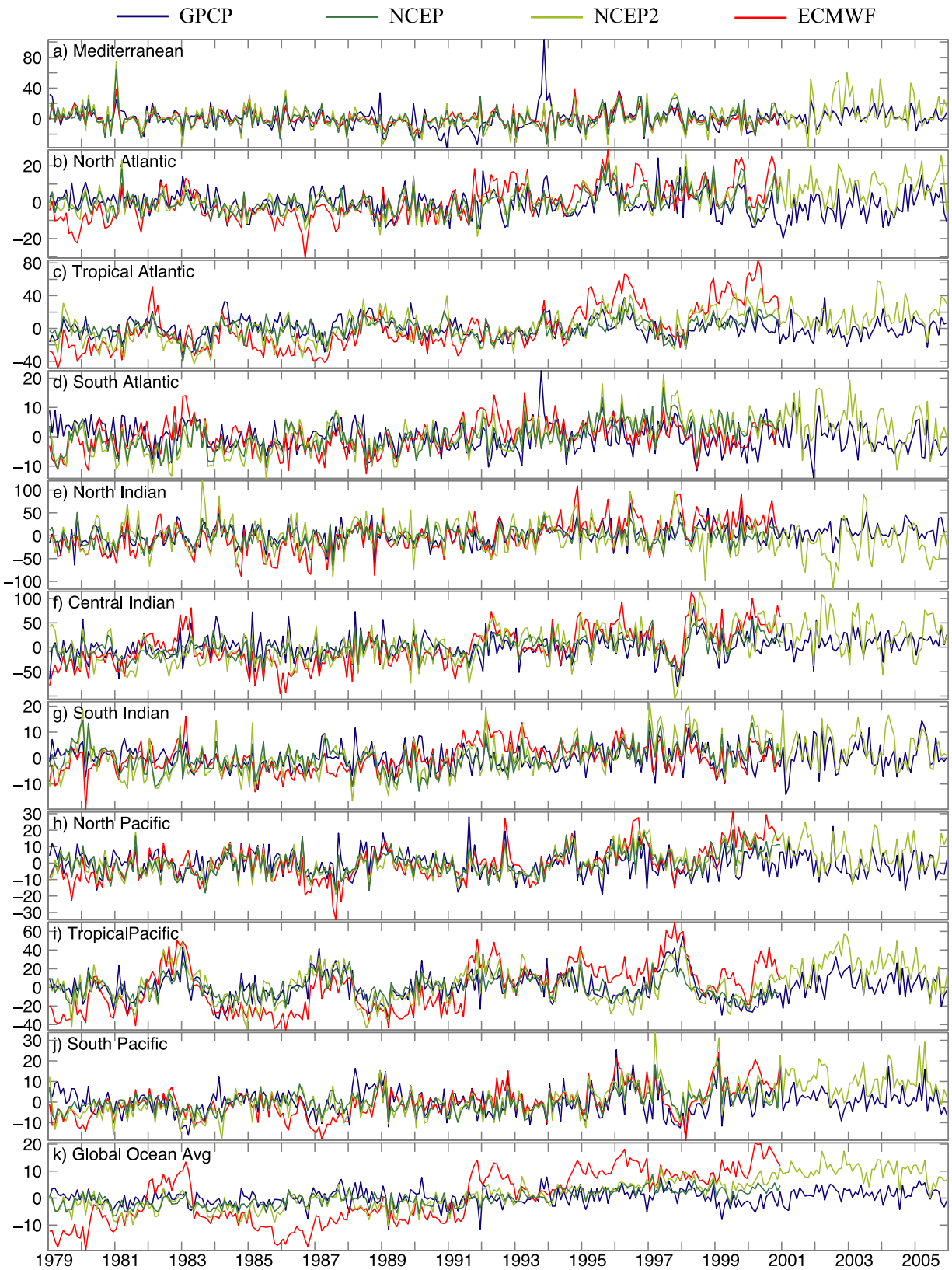
Figure 9. Monthly anomalies for each of the chosen regions. Labels on *x* axis mark starts of years.

and has a minimum (50% less) in August, but then such records would be expected to lag the precipitation extrema.

[22] Although there is a good match in the seasonal averages for the whole Mediterranean, the data sets differ in their associated spatial patterns (Figure 7). All agree on a very dry May to August, with several showing just a little precipitation off eastern Spain and to the north of Corsica. However, the patterns of rainfall in November–December

Table 2. Magnitude of Rainfall Values for all the Regions (in mm Month^{-1})[a]

Region	GPCP Mean	GPCP Season	GPCP Anom	NCEP Mean	NCEP Season	NCEP Anom	NCEP2 Mean	NCEP2 Season	NCEP2 Anom	ECMWF Mean	ECMWF Season	ECMWF Anom
Mediterranean	40.8	18.5	14.0	37.8	22.2	12.1	41.1	20.9	14.3	29.5	17.6	10.0
North Atlantic	79.3	17.7	6.8	78.9	20.3	6.2	84.0	22.5	7.2	83.3	15.5	9.6
Trop. Atlantic	68.4	9.4	12.2	86.1	10.6	11.0	102.4	15.1	17.8	115.7	13.3	26.3
South Atlantic	75.8	6.2	4.8	59.8	8.7	4.9	65.6	10.8	5.8	61.3	5.7	5.1
North Indian	91.3	33.5	22.8	123.9	45.7	18.2	136.7	56.3	33.0	155.0	51.8	35.1
Central Indian	122.7	30.0	26.4	162.1	26.5	20.6	196.6	58.0	35.3	198.1	53.8	37.9
South Indian	70.4	9.6	4.3	64.4	11.3	5.2	77.8	13.4	6.9	64.0	7.8	5.5
North Pacific	85.8	11.6	7.6	88.7	17.9	7.3	95.6	20.8	8.0	91.0	15.6	10.2
Trop. Pacific	122.5	5.0	15.9	143.2	6.3	11.0	177.8	18.4	18.1	197.5	6.3	25.1
South Pacific	82.2	8.2	6.8	74.5	10.0	4.9	89.1	9.3	7.2	77.7	8.6	7.5
Global Ocean	88.0	1.7	2.9	91.5	1.9	2.9	107.3	1.8	4.6	106.5	1.8	9.7

[a]For each data set, the first column gives the mean, the second the r.m.s. variations due to the average seasonal signal, and the third column the interannual variability (r.m.s. variability about the monthly means). All statistics calculated over the common period, 1979–2000.

and January–February are fairly different, with GPCP and ECMWF showing the precipitation to be mainly in the northern part (north of 40°N in the western Mediterranean, and north of 35°N for regions east of 10°E), with the two NCEP reanalyses having rainfall predominantly in the central and eastern parts, and also further south.

[23] The separate removal of the annual precipitation cycle from all four data sets markedly reduces the correlation of GPCP with the models (0.39 with NCEP, 0.47 with NCEP2, and 0.54 with ECMWF), but the correlation between any two different forecast models still remains high (at least 0.82). These monthly anomalies differ by up to 30 mm month^{-1}, although they are in general agreement to within 10 mm month^{-1}. However, larger discrepancies exist in particular in 1981, in late 1993 and the period 1990 to 1992. For 1981 both versions of NCEP indicate anomalies as large as 70 mm month^{-1} while ECMWF indicates 40 mm month^{-1} and GPCP indicates values around 20 mm month^{-1}. Note that the actual values of ECMWF and GPCP are the same in Figure 6a and it is the removal of the seasonal cycle that causes the difference between these two data sets. GPCP appears to have an extremely high value for November 1993; although probably erroneous, it is flanked by other anomalies of ~30 mm month^{-1}, which are not apparent in any of the reanalysis fields.

[24] However, the most interesting discrepancy relates to the period 1990 to 1991. This is the period when deep-water formation in the Eastern Mediterranean took place in the Southern Aegean rather than the Adriatic [*Roether et al.*, 1996], a phenomenon termed the Eastern Mediterranean Transient (EMT). *Roether et al.* [1996] estimated that the observed change in salinity of the dense waters would require an increase in E-P of 1600 mm over the period between the cruises (1987 and 1995) in order to be explained solely by altered surface forcing. However, *Tsimplis et al.* [1997] estimate that only half that increase is required. *Theocharis et al.* [1999] proposed that the colder and drier than usual winters of the early nineties were the reason for the deep-water formation, whereas *Josey* [2003] suggested the cause was reduced heat fluxes as revealed by the NCEP and SOC flux climatologies. However, modeling efforts were unsuccessful in reproducing the EMT until local precipitation and temperature data were assimilated [*Nittis et al.*, 2003]. *Nittis et al.* [2003] specifically refer to the dry period 1989–

1992. Of our data sets, it is only GPCP that shows a large discrepancy from the baseline variability during this period (amounting to ~300 mm less precipitation averaged over the whole Mediterranean, rather than just the eastern part), a finding supported by in situ data [*Tselepidaki et al.*, 1992; *Theocharis et al.*, 1999]. Thus we argue that the production of the EMT indicates that GPCP is probably more accurate during this period.

[25] This analysis is repeated for a further nine regions (as displayed in Figure 5) plus an average over all the oceans; with the different annual cycles shown in Figure 8, the resultant anomalies in Figure 9, and the statistics for each region given in Table 1.

3.1. Seasonal Cycles

[26] Each point on the seasonality plots in Figure 8 represents the mean of 22 individual years. The standard deviation of each set of observations will encompass both the random fluctuations according to whether the satellite pass or ground measurement occurred in the peak or lull of a storm, plus the interannual variability. The standard error in the estimation of the mean is determined by dividing the standard deviation by $\sqrt{(22-1)}$; the resultant value is typically a few percent of the mean rainfall, with the uncertainty in the mean indicated by the dashed lines in Figure 8. This measure is a higher proportion of the mean for ECMWF in the tropical regions (because of the long-term interannual change depicted in Figure 4) and also for GPCP and NCEP in the North and Central Indian, and the Tropical Pacific (three of the main regions affected by El Niño). However, in many cases, the uncertainties in the different data sets do not overlap; i.e., they are significantly different, with one biased high with respect to another. Such a bias represents the relative difference in rain rate according to model or spacecraft sensor of choice; these differences can change their effect through the year. Table 2 gives the magnitude of the annual mean rainfall for each region; the root mean square (r.m.s.) variation due to the seasonal cycle displayed in Figure 8, and the interannual variability about these monthly means. Figure 8a shows that the offset in values for the Mediterranean between ECMWF and both GPCP and NCEP2 is statistically significant (at the 95% confidence level) for most of the year.

3.1.1. Northern Regions

[27] There is a common pattern in most of the northern regions. All four data sets show that the North Atlantic

mean during April-July has at least 30% less rainfall than at the end of the year. The seasonal cycle is enhanced in the latest version of NCEP, with the minimum as for the original version, but the maximum, which occurs in December, increased by ~15 mm month^{-1}. In contrast, ECMWF has its peak rainfall in October. For the North Pacific, GPCP and ECMWF show March-May rainfall reduced by ~30% against the late autumn value, although ECMWF has its seasonal peak in August. Both NCEP data sets show more pronounced minima and maxima compared with GPCP, but agree with it that peak precipitation rates occur in November or December.

[28] The North Indian Ocean is somewhat different because of the monsoon: GPCP and ECMWF show rainfall during February–March to be a minimum with only approximately one third of the rainfall for May–November (southwest monsoon). The NCEP reanalyses shows a similar change, but with their minima and the onset of their peaks delayed by a month or two, and the intensity of their rainfall waning during the summer months. Again, NCEP2 has a larger and later peak than NCEP. Geographical plots of the mean precipitation for each calendar month (not shown) reveal that during the southwest monsoon GPCP, NCEP, and ECMWF all show a region of minimal rain over Sri Lanka, with the region being much broader for GPCP. In contrast, NCEP2 marks this dry period with much heavier rains there than normal. For both the North Indian and the North Pacific, the uncertainty (inter-annual variability) of the ECMWF reanalyses is greater in the second half of the year than the first.

3.1.2. Southern Regions

[29] Unsurprisingly, the three southern regions have different timing for their maxima and minima compared with the northern regions; they also show some differences in the relative performances of the data sets. The GPCP and ECMWF curves show peaks between February and May (austral autumn), and the peaks for these two data sets never differ by more than a month; the NCEP and NCEP2 curves peak between April and June, sometimes two or more months later than the other data sets. For NCEP and NCEP2, the minima are approximately 6 months before the maxima, whereas for GPCP the difference is typically only 4 months, with a sharp increase in monthly rainfall during the start of the year, and a gradual tail off after the peak.

[30] The GPCP data show greater rainfall than NCEP and ECMWF for all three regions (whether expressed as peak month or annual mean); however, NCEP2 exceeds the GPCP values in the South Indian and South Pacific Oceans. The original NCEP reanalysis has the least rainfall (expressed as driest calendar month or annual mean), with it and NCEP2 having the largest amplitude seasonal cycles. NCEP and ECMWF's lower precipitation rates in the austral regions are certainly partially due to their weak portrayal of the South Pacific and South Atlantic convergence zones (SPCZ and SACZ; see Figures 5b and 5d), whereas these features are more pronounced in NCEP2 and GPCP.

3.1.3. Central Regions

[31] The three tropical regions are very different, although there are some common themes. GPCP has the lowest rainfall in all three regions all year round, with the error bounds on NCEP (the next lowest) having only a little overlap with it (July–October in the Tropical Atlantic). Similarly, ECMWF values are always significantly more than in NCEP, except for 4 months (June to September) in the Central Indian. The large ECMWF values are due to the problems with humidity assimilation alluded to in section 2.4. NCEP2 is intermediate between the other two models in the Tropical Atlantic and Tropical Pacific, and clearly matches ECMWF in the Central Indian; in all three regions it has the greatest seasonal variability (see Table 2). Generally, all four data sets agree on the timing of the seasonal cycle in these central regions.

[32] However, for both the Central and North Indian regions the differences between NCEP and ECMWF vary markedly during the course of the year. The greater seasonal variation of NCEP2 in the Central Indian region matches ECMWF, whereas in the Tropical Pacific its variation is far greater than in the other data sets. Except for NCEP2, the seasonal variations in the Tropical Pacific are quite muted, with the other three data sets concurring on a slight maximum in June–July (and August for GPCP), and a weaker secondary maximum at the end of the year. The June–July maximum is not due to the meridional migration of the ITCZ itself, as its gamut is fully encompassed within our defined "Tropical Pacific" region; rather the increase relates to broadening and intensification of the ITCZ in the eastern Pacific.

3.1.4. Seasonal Variations in ITCZ Position

[33] In the Tropical Atlantic, GPCP, and NCEP2 have a July–September minimum that is not as pronounced as in January–February, whereas NCEP and ECMWF have both minima of similar magnitude (Figure 8e). *Béranger et al.* [2006] find the February minimum to be more pronounced than the August–September one for all their data sets; this is because early in the year the ITCZ partially crosses the Equator, one of the boundaries of their chosen region. Figure 10 shows the spatial extent of the seasonal variations in the Tropical Atlantic, with GPCP having its rainfall most tightly focused in location in July–August, which is when it appears most diffuse in NCEP.

[34] The region of maximum rainfall in GPCP lies at its westernmost position in March–April (when the ITCZ is at its furthest south) and is at its easternmost in July–August. This is behavior that was noted by *Chen et al.* [1997] using a totally independent satellite climatology, based on TOPEX altimeter data. NCEP shows no such zonal oscillation across the Atlantic, but rather a regional maximum over Amazonia for November to June, and separately over West Africa for July to October, with some spill from these regions over neighboring waters. The changes shown by ECMWF match GPCP both in west-east migration, and in the latitude of these maxima; NCEP2 shows some similarities, but the rainfall in July to October remains evenly spaced west-east across the Atlantic, and is usually centered one pixel (2.5°) further south than in GPCP and ECMWF.

[35] We also considered the seasonal variations in the Tropical Pacific (not shown). *Quartly et al.* [1999] had shown that both GPCP and TOPEX portray a "double ITCZ" in the eastern Pacific during March–April, and *Chen et al.* [1997] had also commented on the west-east migration of the intensity peak in the ITCZ during the year. All four data sets analyzed in this paper agree that the intensity peak in the Pacific ITCZ is at its easternmost during July–August; however, the latitudinal position of the ITCZ in NCEP2 is one pixel (2.5°) further south. A secondary ITCZ is hard to
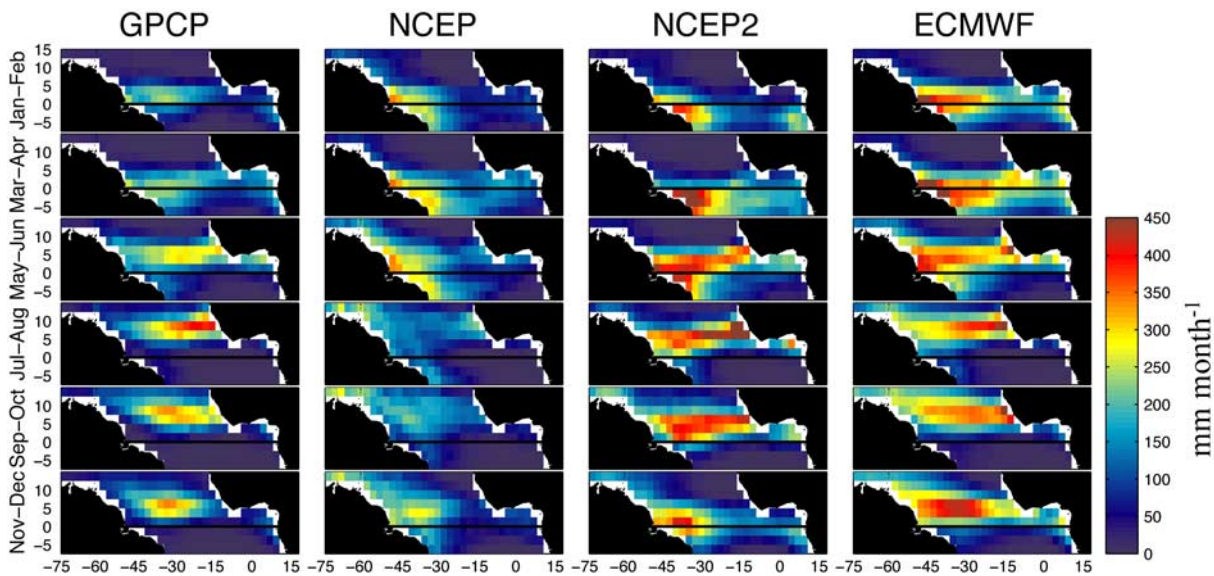
Figure 10. Comparison of seasonal variations of the Atlantic ITCZ, with mean climatologies shown for each 2-month period.

observe in NCEP because of its incorrectly oriented SPCZ, but an eastward extension of the latter is present in March–April. NCEP2 shows a credible representation of this secondary ITCZ, but it is the portrayal in ECMWF that most closely mirrors that of GPCP. *Béranger et al.* [2006] intercompared representations of the double ITCZ using an individual month (March 1993), and for that found it present in all data sets, but better represented in NCEP than ECMWF. However, they were using ERA-15, an earlier version of the ECMWF reanalysis than used here.

3.1.5. Global Average

[36] Finally, we consider the mean precipitation over all the ocean regions (65°S to 65°N). The overall mean for GPCP is 88 mm month^{-1}, with NCEP a little higher, and NCEP2 and ECMWF agreeing on 107 mm month^{-1}. These values represent the uncertainty in global mean precipitation, with no single value known to be correct. *Taylor* [2000] reports that the evaporative rates in all three models exceed that derived from ship estimates; consequently, one might conclude that the precipitation values in the reanalyses are likely to be overestimates. Not surprisingly, the seasonality in all data sets is weak (see Figure 8h and bottom row of Table 2). All the data sets show two seasonal maxima: the models have them in May/June/July and December, whereas GPCP's global precipitation peaks in March and November. *Janowiak et al.* [1998] calculated a mean global precipitation rate over land and ocean, using 7 years of data: their plots show a mean for GPCP of ∼81 mm month^{-1}, and for NCEP of ∼84 mm month^{-1}, with only the latter exhibiting a clear seasonal cycle, with a peak of 90 mm month^{-1} in June. The clear seasonality in our global analysis of GPCP is likely to be a result of rainbands migrating on and off land (where they are clearly not counted within our "global ocean").

3.2. Monthly Anomalies

[37] The monthly anomalies for the four data sets are displayed in Figure 9; note that all are relative to a seasonal

cycle calculated over 1979–2000. The largest r.m.s. variations (see Table 2) are in the three central/tropical regions plus the Mediterranean and North Indian regions. ECMWF has the largest anomalies in four of these regions, which correspond to the regions of significant trend (Figure 4b), although the time series in Figure 9 show it to be far from a simple common trend across all regions. The southern regions of the Atlantic, Indian, and Pacific have smaller seasonal variations than their northern counterparts; they also have smaller interannual variation (only 4.3–7.5 mm month^{-1}, see Table 2).

[38] The correlations of these interannual variations are shown in the right hand columns of Table 1. The regions showing the most coherent variations across all four data sets are the Tropical Atlantic, North Indian, and all three parts of the Pacific, with all their comparisons having correlations exceeding 0.5. These are predominantly regions with a precipitation response to El Niño [*Xie and Arkin*, 1997; *Gruber et al.*, 2000; *Kyte et al.*, 2006]. The three reanalysis fields are also highly correlated for the Mediterranean, probably reflecting the high density of land observations circumscribing this region. For this region, the reanalysis that most agrees with GPCP is ECMWF. The South Indian is the region with the greatest discrepancies; apart from the comparison of NCEP with NCEP2, no pair of climatologies shows a correlation greater than 0.5.

[39] Although the global mean rainfall shows little seasonal variation for any of the climatologies, the interannual variability for ECMWF is much more marked than for the others (Figure 9k), with the changes mainly mirroring the apparent increases in tropical regions (cf. Figures 9c and 9i). Given that there is little variation in the global average rainfall, it is likely that anomalies for each individual data set are more heavily influenced by the errors in the model or satellite algorithm than by real changes in the mean global precipitation over the ocean. Consequently, one might not expect large correlations between data sets for global anomalies.

3.3. Long-Term Changes

[40] Following a referee's suggestion, we have reexamined the seasonal cycles for each region separating the data into pre-1991 and post-1991. For GPCP the long-term changes were minor: Mediterranean winters were drier by about 10 mm month^{-1}, and over the North Indian region rainfall rates increased by 10 to 15 mm month^{-1} during the southwest monsoon. For all other regions the differences in monthly precipitation between the two periods were of order 2%. This absence of a trend on both an annual and a monthly basis implies the GPCP has high internal consistency. It is possible that this uniformity is partially an enforced one, through the calibration procedures applied to each separate satellite generating the instrument-specific products. By applying an EOF analysis, *Smith et al.* [2004] uncovered a weak increasing trend in GPCP over large sectors of the ocean; however, they still concluded that the global mean change was near zero.

[41] For ECMWF, an increase occurs between pre-1991 and post-1991 in all regions except for the Mediterranean. The change was of order 5% for the southern basins, and 20% for the northern and central basins, except the Tropical Atlantic which had a 30% increase. Like GPCP, there was minimal change to the seasonal profile in each region. The changes for NCEP and NCEP2 were less than for ECMWF, with five regions (northern basins, Mediterranean, and Tropical Pacific) showing no change. The seasonal increases were similar for NCEP and NCEP2, with the southern basins receiving their extra rainfall during the wet season early in the year, and the Central Indian having its increase during the drier part (April to August). In the Tropical Atlantic, NCEP increased by ∼10% during April–June, whereas NCEP2 increased by 15–20% for the whole of the April to October period.

[42] From these analyses, it can be seen that the various data sets diverge with respect to the changes in the Tropical Atlantic, with GPCP showing no long-term change, ECMWF having a 30% increase year round, and the two different NCEP reanalyses showing their greatest differences in derived trends. Consequently, the Tropical Atlantic appears to be a pivotal region for reconciling the long-term variations seen within these different data sets.

4. Discussion

[43] There are a large number of precipitation climatologies, which differ in their magnitude and their representation of seasonal variations. We have analyzed four of them here, specifically concentrating on long duration data sets and the differences between satellite and reanalysis fields. In this section we discuss our findings in the light of others' results.

4.1. Use of GPCP as a Reference?

[44] Clearly, there is no universally-agreed reference data set for precipitation, although one based upon satellite data would be expected to get the geographical locations of precipitation correct. Over the ocean there are different SSM/I algorithms according to whether the inversion is based upon emission of low-frequency microwaves or scattering of high frequencies (37 and 85 GHz), plus there are algorithms based upon the infrared signatures of clouds.

For example, another widely used satellite-based data set is CMAP (Climate Prediction Center Merged Analysis of Precipitation, see *Xie and Arkin*, 1997), which uses both SSM/I-scattering and SSM/I-emission algorithms over the ocean, whereas GPCP only uses the latter, but also incorporates TOVS at higher latitudes. CMAP also has a different merging procedure [*Gruber et al.*, 2000]. The standard CMAP analysis does incorporate reanalysis output in poorly observed areas, which tend to be around the poles and thus have little impact on the comparisons discussed here.

[45] Because of their use of principally the same satellite sensors, the positioning of rain features in the two data sets agrees very well; however, the intensity of features differs on account of the different algorithms employed. The global mean oceanic precipitation in GPCP and CMAP agree to within a few percent, but the correlation between the two series is only 0.36 [*Yin et al.*, 2004], similar to that for GPCP with either of the NCEP reanalyses (bottom row of Table 1). CMAP has a precipitation rate ∼10% higher than GPCP in the tropics (which is believed to be due to CMAP's overreliance on sparse atoll data [*Yin et al.*, 2004]), and ∼10% less in the midlatitudes [*Gruber et al.*, 2000], but the temporal variations of the two at each location are highly correlated (see Figure 10 of *Xie and Arkin* [1997]). *Gruber et al.* [2000] note that, averaged over the entire northern hemisphere, CMAP has a greater rain rate than GPCP from April to November, with the reverse for the rest of the year. Although the magnitude of their areal averages differ, *Béranger et al.* [2006] find very good agreement between CMAP and GPCP in terms of their seasonal cycle, the main difference being the greater range shown by CMAP in the equatorial Pacific. GPCP and CMAP also agree closely on the positioning and magnitude of the precipitation anomaly associated with the 1997/1998 El Niño (Figure 12 of *Gruber et al.* [2000]).

[46] There are considerable uncertainties as to the true latitudinal distribution of rain, for example *Kakar and Kummerow* [2000] showed that early climatologies based on different instruments on the same satellite differed by 30% in the tropics. *Janowiak et al.* [1998] were concerned about the relatively high precipitation rates shown by GPCP in the northern storm tracks, but concluded that these were realistic or even an underestimate of the true situation. Another widely used satellite data set is based on the Microwave Sounding Unit (MSU, Spencer, 1993). However, *Béranger et al.* [2006] concluded that the MSU showed too much rainfall in the storm-track regions, and had seasonal cycles in many regions that were markedly different to that shown by other data sets.

[47] In conclusion, there is no clear consensus on the absolute magnitude of precipitation in the tropical and midlatitude bands; GPCP shows spatial patterns of precipitation similar to other satellite-based data sets, agrees with CMAP on the magnitude of changes associated with El Niño and has a high degree of internal consistency as shown by the minimal regional trends (section 3.3) and the constancy in variability since 1987 (Figure 2). However, the ultimate decision as to the best precipitation data set for climate studies *per se*, or for forcing of ocean models, awaits a reliable determination of absolute magnitudes.

4.2. Comparison of Mean Precipitation Fields

[48] Although each of our chosen data sets has its own deficiencies, we are interested in seeing how much they agree upon aspects of regional average rainfall. To this end, we have calculated mean absolute rainfall, seasonal cycle, and interannual variability for each region and each data set (see Table 2). For many regions time series of the four different rainfall estimates show superficially good agreement. Closer investigation indicates that many of the estimates of the mean differ by more than 10%. The ECMWF precipitation values in the region 30°S to 30°N have increased markedly with time (Figure 4), and consequently the ECMWF mean is up to 50% higher than the others in these regions. This is due to the increased reliance upon satellite observations of humidity [*Uppala et al.*, 2004]. *Hagemann et al.* [2005] note that not only does the ECMWF precipitation over the ocean increase, but it also continues to exceed the flux to the atmosphere via evaporation.

[49] Values of mean rainfall as a function of latitude show a strong peak at 6°N corresponding to the mean position of the ITCZ, and a weaker secondary peak at 8°S, principally due to the SPCZ. Local minima exist at 20°S and 20°N, with further midlatitude peaks at ∼40°S and ∼40°N corresponding to the midlatitude storm tracks. Both *Taylor* [2000] and *Béranger et al.* [2006] found the principal tropical peak to be 20–30% larger in CMAP than in NCEP, with ERA-15 being greater still. *Taylor* [2000] also noted NCEP2 to be 10% greater and considered this to be "too large". NCEP overestimates winds at low wind speed and underestimates high ones, especially for the meridional component [*Taylor*, 2000]. The resulting weaker convergence of the wind field explains why NCEP shows the precipitation signal in the ITCZ to be broader than in other climatologies.

[50] On the other hand, GPCP has higher estimates than NCEP and ECMWF in all three southern regions, which is mainly due to those models' poor rendition of the SPCZ and SACZ, which has been improved in NCEP2. *Kistler et al.* [2001] noted that the southern midlatitude rain belt is located at ∼50°S in both NCEP and the ERA-15, whereas the belt is at 35°S in both CMAP and GPCP. *Yin et al.* [2004] find another GPCP peak at ∼60°S, where its mean rain rate of 100 mm month^{-1} is more than twice that shown by CMAP. For some data fields within weather forecast models, the accuracy in the southern hemisphere is now comparable with that in the better-instrumented northern half (see for example, Figure 15 of *Uppala et al.* [2004]). This does not seem to be the case for precipitation, where the mispositioning of some rainbands points to errors in the strength and positioning of the convergence cells. *Janowiak et al.* [1998] observed that where the SPCZ joined the western end of the Pacific ITCZ there was a local minimum in NCEP precipitation that was not shown in GPCP. Our analysis for a much longer period does show this equatorial feature in GPCP, NCEP, and ECMWF, but surprisingly not in NCEP2.

4.3. Comparison of Seasonal Cycles

[51] While there have been a number of papers that compare satellite and reanalysis fields in terms of their mean spatial distribution, their latitudinal profiles, and their response to El Niño, far fewer published papers have looked at their seasonal cycle. In our analysis (Figure 8 and Table 2), NCEP showed larger seasonal variations than GPCP or ECMWF in seven of the regions (with the ECMWF annual cycle being larger in the Tropical Atlantic and North and Central Indian). GPCP often showed the weakest seasonality. However, the seasonal cycle in NCEP2 exceeded that of NCEP in eight of the regions, in three of the cases by more than 40%, confirming results of an initial analysis of 5 years' data (Figure 11.4.36b of *Taylor* [2000]). Strangely, NCEP's representation of the seasonal cycle often peaked a month or more later than in the GPCP or ECMWF (Figure 8), with NCEP2 doing likewise or being later still. NCEP and NCEP2 also showed very different seasonal patterns to the others in the North Indian region during the southwest monsoon.

[52] *Janowiak et al.* [1998] compared GPCP and NCEP for two large regions (each 40° by 60°), and noted that for both NCEP had the larger mean and the larger seasonal variation. These two regions, both predominantly over land, showed no difference between the two data sets as regards the phase of their seasonal cycles. Using CMAP as a reference, *Béranger et al.* [2006] also noted that the phasing of NCEP was a month or two later for parts of the North Pacific, the western Indian, the South Indian and the southwest Atlantic (their Figure 6).

4.4. Interannual Variations and the Detection of Trends

[53] For most regions the output of NCEP and NCEP2 are highly correlated, whether considering absolute precipitation or anomalies (see Table 1). In pair-wise comparisons of the anomalies in the other data sets, the correlations are moderate (0.4 to 0.7), although statistically significant. The regions of highest correlation are those associated with a precipitation response to El Niño. Given the relatively low correlations, it is initially surprising that an investigation of the interannual changes associated with El Niño and the North Atlantic Oscillation shows good agreement between the data sets in terms of the spatial patterns and magnitudes of their responses [*Kyte et al.*, 2006]. This is because both these phenomena essentially redistribute the precipitation rather than increase it. Therefore if the oceanic regions are chosen appropriately, the net changes over them are not large, and the areal anomalies portrayed in different data sets are only moderately correlated.

[54] The question as to whether there is long-term change in oceanic precipitation, for example, a response to global warming, is hard to address with any of these data sets. All three reanalysis data sets have anomalous behavior within the era studied, including step changes in areal averages (Figure 3) and trends unsupported by the satellite observations (Figure 4). A simple division into the pre-1991 and post-1991 epochs shows increases of order 10–20% in the reanalyses for some regions. However, the satellite data are much more consistent, especially from July 1987 onwards (see Figure 2), and appear more believable in this context. The long-term increase in ECMWF (Figure 9k) is attributable to problems with humidity assimilation; the increase for NCEP2 in the last 5 years is not understood. *Mitas and Clement* [2005] discovered that ERA-40 and the first NCEP reanalysis show an increase in the intensity of the tropical

Hadley cell circulation (i.e., the meridional overturning of the atmosphere) that is not borne out by the analysis of rawinsonde observations. However, these trends in the reanalyses are also present in the period before satellite data were ingested into the models. *Kistler et al.* [2001] specifically caution users against long-term studies using NCEP without taking account of all the changes in the observing system.

4.5. Forcing of Ocean Models

[55] A precipitation climatology is an important part of the forcing for ocean models. In this paper we have not looked at the evaporative component of the freshwater flux, as again a number of different estimates exist for that. When considering many combinations of precipitation and evaporation data sets, *Sohn et al.* [2004] found the effect of uncertainties in the former to be greater, with the largest disagreements in the zonal flux of water vapor corresponding to the wide range of precipitation estimates over the western Pacific warm pool area.

[56] The use of precipitation climatologies as part of the forcing in ocean models is not straightforward, given the level of uncertainty in these data sets. Many models include a "relaxation term" to restore surface salinities toward observations, typically a monthly climatology, for example, *Levitus et al.* [1998]. This "correction" is needed to overcome the model drift that may arise from a persistent freshwater excess or deficit, but will also serve to mask real salinity changes due to atypical forcing such as El Niño. Secondly, models often apply a global multiplier to their chosen precipitation climatology to help minimize the relaxation in a global context. This multiplier may then be changed at the start of each model year; see *Yeager and Large* [2004] for further details. Again, this is a very broad-brush approach, adjusting all regions when the erroneous estimates may only be in one region, and applying it throughout the year when the problems with the data might be for only the dry or the wet season.

[57] A consequence of this is that the key parameter for selecting a forcing data set is not the mean global precipitation, but rather the relative distribution of rainfall between different regions. For this the "truth" is not really known, but a first choice would be one that broadly matches the distribution shown by land-based rain gauges. However, both CMAP and GPCP take notice of such data, and yet their ratios of precipitation in midlatitudes to tropics differ by 25%. The other important factor is consistency, which would point to GPCP being the first choice among the climatologies evaluated here. However, it would be a very instructive exercise to run the same model with different forcing fields to test sensitivity (this is currently being done by colleagues at NOC; B. de Cuevas, personal communication, 2006).

4.6. Relative Merit of Reanalysis Fields

[58] All three reanalysis climatologies show roughly the correct patterns of precipitation (Figure 5), and all show greater rain rates in the tropics than in GPCP, and NCEP and ECMWF show less than GPCP in the midlatitudes. (A slightly different view is taken, if CMAP is used as the reference). ECMWF has a well-documented increase in precipitation during that period, leading *Troccoli and Kållberg* [2004] to suggest a blanket correction toward a mean GPCP climatology, and others to impugn that the ECMWF precipitation data set has no use. The time-varying bias in ECMWF precipitation values is certainly pronounced in any study of interannual variations spanning the tropics (see Figure 9). However, of the three reanalysis fields studied here, it is the best at replicating the position of the ITCZ, the secondary band in the Pacific during March–April, the west-east migration of activity in both the Atlantic and Pacific ITCZ, and the patterns of rainfall in the Mediterranean.

[59] NCEP and ECMWF differ in the nature of the underlying model, the method of assimilation, and the types of data used. While ECMWF started incorporating high-resolution vector wind data from scatterometry from 1993 onwards, NCEP has not done so. Therefore the advent of active microwave sensors on satellites cannot explain the change in NCEP data noted for 1991 onwards (Figure 3). To resolve the causes of the discrepancy between models would require that each of the models be run for several years, with different options as to the data assimilated. Even with today's computers, that would be an intensive task given the number of realizations and years required.

[60] The change in model from NCEP to NCEP2 included various improvements in the physics, with one of the results being an increase in the latitudinal profile of precipitatble water to match the NVAP climatology better [*Kanamitsu et al.*, 2002]. The change led to an improved orientation of the SPCZ, but also a southward shift of the ITCZ. However, the largest effect has been to increase the mean precipitation field (by 16% for the global ocean, see Table 2), enhance the seasonal cycle in most regions (Figure 8), and make the interannual variability significantly larger (Table 2). It also maintains the errors in the seasonal cycle noted previously for NCEP [*Béranger et al.*, 2006], and for the area around Sri Lanka shows considerable rain during the dry season (section 3.1.1).

5. Summary

[61] A knowledge of the oceanic rainfall is important because of the impact of net freshwater flux upon surface salinity and hence ocean circulation. In analyzing and comparing these four well-established climatologies, there is no absolute reference; the satellite-based data sets cannot simply be assumed to be quantitatively correct, and alternative climatologies such as those based upon ship observations have large measurement and sampling errors too. However, it is reasonable to assume that a precipitation data set based on satellite observations will correctly indicate the spatial distributions of precipitation. Thus although each of our chosen data sets has its own deficiencies, we are interested in seeing how much they agree upon aspects of regional average rainfall, illustrating their differences with the aim of inspiring those working on the development of models and satellite climatologies to address these issues, and commenting upon the appropriateness of such data sets for forcing ocean models.

[62] All four data sets analyzed here show internal inconsistencies (Figures 2, 3, and 4), which may not be surprising given the changes in the nature and the quantity of their various source data (Figure 1). For GPCP, the change in the character of the data set after the inclusion of SSM/I only appears to affect the variability, whereas for some locations NCEP and NCEP2 show step changes in their mean values.

The increase in ECMWF precipitation with time has been well-documented (e.g., *Uppala et al.*, 2004); however, Figure 4b shows the areal extent of the effect, and the relevant parts of Figure 9 show that the change with time is not a simple trend.

[63] While at first glance the patterns of the mean precipitation fields are similar in all four data sets (Figure 5), there are marked differences in the magnitude of the Pacific ITCZ and the North Atlantic and North Pacific storm tracks, as well as in the location of features such as the SPCZ. The differences for the Mediterranean and the Atlantic ITCZ are enhanced when individual parts of the seasonal cycle are considered. Of the three reanalysis fields considered, only ECMWF gets the spatial distribution of rain in the Mediterranean correct, and only it shows a clear west-east migration of the intensity peak in the Atlantic ITCZ (Figure 10).

[64] The four data sets were analyzed in terms of their mean freshwater input over selected regions, which is appropriate for the forcing of ocean models or the study of climatic changes. In analyzing six data sets for 1980–1993, *Béranger et al.* [2006] noted that, with the exception of NCEP, most agreed on the phasing of the seasonal cycles, but often differed in amplitude. Our analysis here, using more recent versions of the satellite and reanalysis data sets and a longer analysis period, principally concurs. However, we note that in northern and southern regions the seasonal cycle of NCEP is usually a month behind GPCP and ECMWF, with NCEP2 often being later still. The revision to the NCEP model has increased the mean precipitation field, its seasonal range, and the size of variations about the seasonal cycle (Figures 8 and 9 and Table 2). However, it is very much based upon the same model, so although there are changes in magnitude, and improvements in the positioning of the SPCZ, it is not surprising that their areal averages are highly correlated (Table 1).

[65] While the GPCP data set does have the occasional anomalous month for the Mediterranean, it is the only one to suggest a marked deficit in rain over 1990–1991, consistent with local observations. Thus GPCP is the only data set to hint at the changes in forcing needed to shift deep-water formation during the Eastern Mediterranean Transient.

[66] In general, there is greater correlation between any two numerical weather forecast models than for one of them with the satellite data set; this is not surprising given the considerable overlap in the sources of data employed by the models. For most of the Atlantic and Pacific regions, GPCP showed higher correlation with NCEP and NCEP2 than with ECMWF. However, for all three parts of the Indian Ocean, it is the NCEP2 reanalysis that has the least correlation with GPCP. The largest interannual anomalies and the strongest correlations of data set anomalies were mainly found for the regions associated with El Niño and La Niña. Despite the North Atlantic Oscillation having a marked effect upon the spatial distribution of precipitation, once the North Atlantic is taken as a whole the size of interannual variations and the correlations between data sets are no greater than for most other regions. Indeed, when considering the mean for the global ocean, there is only a weak correlation between the satellite- and model-derived data sets.

[67] To give the correct freshwater forcing for ocean models, it is not the total global precipitation that matters, but rather the distribution between different oceanographic regions, both in terms of ratio between midlatitudes and tropics, and as to whether in Indian, Atlantic or Pacific Oceans. Although a data set based on satellite observations would be an obvious choice, it is not clear that it gets the latitudinal profile of precipitation correct, given the changes in sensor technology used for different latitudinal bands, and the progression from convective to stratiform systems. Another important factor is the consistency of the data set; of those studied here, GPCP showed the most stability with time. Another desirable attribute would be that the chosen data set adequately portrays interannual variations. *Kyte et al.* [2006] showed that there was a lot of agreement between these data sets concerning the changes associated with El Niño and the North Atlantic Oscillation. In our analysis here we suggest that GPCP may be the only one to portray the necessary rainfall deficit to cause the EMT. Taking these points together, we believe that GPCP would be the best choice for providing freshwater fluxes, but would also recommend studies to see how sensitive ocean models are to the choice of forcing field.

[68] Overall, there are subtle variations between the climatologies in mean rainfall rate, representation of seasonal cycle, and interannual variations, with different disagreements occurring in different regions. Since we have demonstrated that each climatology has its own particular artifacts, caution should always be exercised in interpreting anyone's conclusions about changes in the freshwater flux into the ocean if they are based solely upon analysis of a single data set. For the reanalysis data sets, one means of determining the causes of their disagreements (underlying model, data used or assimilation scheme) is to perform limited runs using the same data sources. Further diagnostic work could be achieved by classifying the rain into frontal and convective activity, according to the associated wind field, but that would probably require the use of 6-hourly data and the use of a satellite wind data set that does not suffer from contamination by rain. Uncertainties as to the true latitudinal distribution of rainfall still exist, with the two main composite satellite products (GPCP and CMAP) differing in the algorithms and weighting to be applied to the various passive microwave and infrared data sets. It is to be hoped that the considerable effort on ground validation for TRMM, and the extra information provided by its precipitation radar (between 37°S and 37°N) will improve the accuracy of other satellite data sets.

References

Adler, R. F., C. Kidd, G. Petty, M. Morissey, and H. M. Goodman (2001), Intercomparison of global precipitation products: The third precipitation intercomparison project (PIP-3), *Bull. Am. Meteorol. Soc.*, 82, 1377–1396.

Adler, R. F., et al. (2003), The version-2 Global Precipitation Climatology Project (GPCP) monthly precipitation analysis (1979–present), *J. Hydrometeor.*, 4, 1147–1167.

Béranger, K., B. Barnier, S. Gulev, and M. Crépon (2006), Comparing 20 years of precipitation estimates from different sources over the world ocean, *Ocean Dyn.*, 56, 104–138, doi:10.1007/s10236-006-0065-2.

Chen, G., B. Chapron, J. Tournadre, K. Katsaros, and D. Vandemark (1997), Global oceanic precipitation: A joint view by TOPEX and the TOPEX microwave radiometer, *J. Geophys. Res.*, *102*(C5), 10,457–10,471.

Gruber, A., X. Su, M. Kanamitsu, and J. Schemm (2000), The comparison of two merged rain gauge-satellite precipitation datasets, *Bull. Am. Meteorol. Soc.*, *81*, 2631–2644.

Hagemann, S., K. Arpe, and L. Bengtsson (2005), Validation of the hydrological cycle of ERA-40, ERA-40 Project Report Series, 24.

Huffman, G. J., et al. (1997), The global precipitation climatology project (GPCP) combined precipitation data set, *Bull. Am. Meteorol. Soc.*, *78*, 5–20.

Huffman, G. J., and D. T. Bolvin (2004), GPCP version 2 combined precipitation data set documentation, ftp://precip.gsfc.nasa.gov/pub/gpcp-v2/doc/.

Janowiak, J. E., A. Gruber, C. R. Kondragunta, R. E. Livezey, and G. J. Huffman (1998), A comparison of the NCEP-NCAR reanalysis precipitation and the GPCP rain gauge-satellite combined dataset with observational error considerations, *J. Clim.*, *11*, 2960–2979.

Josey, S. A. (2003), Changes in the heat and freshwater forcing of the eastern Mediterranean and their influence on deep water formation, *J. Geophys. Res.*, *108*(C7), 3237, doi:10.1029/2003JC001778.

Kakar, R., and C. Kummerow (2000), The tropical rainfall measuring mission (TRMM)—What have we learned and what does the future hold? Proc. of PORSEC '00, Goa, India, 5th–8th Dec. 2000, vol. I, pp 138–142.

Kanamitsu, M., W. Ebisuzaki, J. Woollen, S.-K. Yang, J. J. Hnilo, M. Fiorino, and G. L. Potter (2002), NCEP-DOE AMIP-II reanalysis (R-2), *Bull. Am. Meteorol. Soc.*, *83*, 1631–1643, doi:10.1175/BAMS-83-11-1631.

Kidd, C. (2001), Satellite rainfall climatology: A review, *Int. J. Climatol.*, *21*, 1041–1066.

Kistler, R., et al. (2001), The NCEP-NCAR 50-year reanalysis: Monthly means CD-ROM and documentation, *Bull. Am. Meteorol. Soc.*, *82*, 247–267.

Kyte, E. A., G. D. Quartly, M. A. Srokosz, and M. N. Tsimplis (2006), Interannual variations in precipitation: The effect of the North Atlantic and Southern Oscillations as seen in a satellite precipitation data set and in models, *J. Geophys. Res.*, *111*, D24113, doi:10.1029/2006JD007138.

Levitus, S., T. Boyer, M. Conkwright, D. Johnson, T. O'Brien, J. Antonov, C. Stevens, and R. Gelfeld (1998), Introduction. World Ocean database 1998, vol. 1, NOAA Atlas, NESDIS 18, US Government Printing Office, 346 pp.

Mass, C. F., and D. A. Portman (1989), Major volcanic eruptions and climate: A critical evaluation, *J. Clim.*, *2*, 566–593.

Mitas, C., and A. Clement (2005), Has the Hadley cell been strengthening in recent decades?, *Geophys. Res. Lett.*, *32*, L03809, doi:10.1029/2004GL021765.

Nittis, K., A. Lascaratos, and A. Theocharis (2003), Dense water formation in the Aegean Sea: Numerical simulations during the Eastern Mediterranean Transient, *J. Geophys. Res.*, *108*(C9), 8120, doi:10.1029/2002JC001352.

Quartly, G. D., M. A. Srokosz, and T. H. Guymer (1999), Global precipitation statistics from dual-frequency TOPEX altimetry, *J. Geophys. Res.*, *104*, 31,489–31,516.

Quartly, G. D., T. H. Guymer, and K. G. Birch (2002), Back to basics: Measuring rainfall at sea: Part 1. In situ sensors, *Weather*, *57*, 315–320.

Roether, W., B. B. Manca, B. Klein, D. Bregant, D. Georgopoulos, V. Beitzel, V. Kovacevic, and A. Luchetta (1996), Recent changes in eastern Mediterranean deep waters, *Science*, *271*, 333–335.

Smith, T. M., X. Yin, and A. Gruber (2004), Variations in annual global precipitation (1979–2004), based on the Global Precipitation Climatology Project 2.5° analysis, *Geophys. Res. Lett.*, *33*, L06705, doi:10.1029/2005GL025393.

Sohn, B. J., E. A. Smith, F. R. Robertson, and S. C. Park (2004), Derived over-ocean water vapor transports from satellite-retrieved E-P datasets, *J. Clim.*, *17*, 1352–1365.

Struglia, M. V., A. Mariotti, and A. Filograsso (2004), River discharge into the Mediterranean Sea: Climatology and aspects of the observed variability, *J. Clim.*, *17*, 4740–4751.

Taylor, P. K. (2000), Intercomparison and validation of ocean-atmosphere energy flux fields, World Climate Research Programme report WCRP-112, 303 pp.

Theocharis, A., K. Nittis, K. Kontoyiannis, E. Papageorgiou, and E. Balopoulos (1999), Climatic changes in the Aegean Sea influence the Eastern Mediterranean thermohaline circulation (1986–1997), *Geophys. Res. Lett.*, *26*, 1617–1620.

Troccoli, A., and P. Kållberg (2004), Precipitation correction in the ERA-40 reanalysis, *ERA-40 Project Report Series*, 13.

Tselepidaki, I., B. Zarifis, and D. Asimakopoulos (1992), Low precipitation over Greece during 1989–1990, *Theor. Appl. Climatol.*, *46*, 115–121.

Tsimplis, M. N., A. F. Velegrakis, A. Theocharis, and M. B. Collins (1997), Low-frequency current variability at the straits of Crete, eastern Mediterranean, *J. Geophys. Res.*, *102*(C11), 25,005–25,020.

Uppala, S., P. Kållberg, A. Hernandez, S. Saarinen, M. Fiorino, X. Li, K. Onogi, N. Sokka, U. Andrae, and V. Da Costa Bechtold (2004), ERA-40: ECMWF 45-year reanalysis of the global atmosphere and surface conditions 1957–2002, *ECMWF Newsletter*, *101*, 2–21.

Xie, P., and P. A. Arkin (1997), Global precipitation: A 17-year monthly analysis based on gauge observations, satellite estimates, and numerical model outputs, *Bull. Am. Meteorol. Soc.*, *78*, 2539–2558.

Yeager, S. G., and W. G. Large (2004), Late winter generation of spiciness on subducted isopycnals, *J. Phys. Oceanogr.*, *34*, 1528–1547.

Yin, X., A. Gruber, and P. Arkin (2004), Comparison of the GPCP and CMAP merged gauge-satellite monthly precipitation products for the period 1979–2001, *J. Hydrometeor.*, *5*, 1207–1222.

———————

E. A. Kyte, G. D. Quartly, M. A. Srokosz, and M. N. Tsimplis, National Oceanography Centre, Southampton, Empress Dock, Southampton, Hants SO14 3ZH, UK. (gdq@noc.soton.ac.uk)